Kovove Mater. 49 2011 401–409
DOI: 10.4149/km_2011_6_401

NDT characterization of decarburization of steel after long-time annealing

B. Skrbek[1], I. Tomáš[2]*, J. Kadlecová[2], N. Ganev[3]

[1] *Technical University in Liberec, Studentská 2, 461 17 Liberec, Czech Republic*
[2] *Institute of Physics ASCR, v.v.i., Na Slovance 2, 182 21 Prague 8, Czech Republic*
[3] *Czech Technical University in Prague, Faculty of Nuclear Sciences and Physical Engineering, Břehová 7, 115 19 Prague 1, Czech Republic*

Received 16 December 2010, received in revised form 2 June 2011, accepted 3 June 2011

Abstract

Decarburization is a common adverse effect at manufacturing and processing of steel semi-products. A series of samples of various shapes, produced from spring steel 54SiCr6 (CSN 14260), was prepared and annealed at 800 °C at air atmosphere for 1, 4, 8, and 20 h. The decarburized layers that appeared on the surfaces were examined metallographically and magnetically by Magnetic Adaptive Testing (MAT). The magnetic tests proved an appreciable sensitivity, which depended on the samples shapes, on the way of measurement and on the surface treatment of the samples before the measurement.

Careful weighing of the samples before and after the annealing and/or after the surface treatment proved to be a simple and reliable way for determination the thickness of the decarburized layer as well.

K e y w o r d s: decarburization, spring steel, non-destructive testing, Magnetic Adaptive Testing (MAT), weighing

1. Introduction

Material toughness of surface of industrial structures represents their key protection against fatigue failure. This is the reason why structures exposed to considerable fatigue loads are frequently artificially equipped with surface layers, which substantially exceed fatigue limits of the core material (technological treatments for surface hardening, nitration, strengthening and others).

On the other hand, unwanted decarburization of construction ferrous alloys can generate a *soft* surface layer, depleted of carbon (and sometimes depleted also of other elements, whilst some harmful elements and phases can there appear instead), which *degrades* the industrial properties. The surface decarburization considerably decreases strength and durability of the component as compared with the values of its core.

Common high temperature technological processes of steel and cast iron semi-products like casting, working (forging, rolling...) and any other heat treatment without protective atmosphere are susceptible to decarburization. Any failure of the protective atmosphere control, or pollution (oxidation) of salt austenitizing baths (for instance at treatments of high speed steels and powder metallurgy products) threatens to create decarburized surfaces as well.

Decarburization of steel components takes place even in reduction atmospheres under action of active hydrogen, e.g. in chemical industry. Hydrogen combines with carbon into simple hydrocarbons at the steel surface, and as the used carbon is supplied by diffusion from depth of the material, a decarburized surface layer appears. Diagnostics of surface decarburization can thus also serve as a preventing check-up of selected elements of chemical accessories.

The international standard ISO 3887 reflects importance of the decarburization problem and recommends three reliable ways of detection of this degradation, all of them *destructive*: They are (i) metallographic observation of the increased ferrite ratio in the ferrite/pearlite microstructure, (ii) measurement

*Corresponding author: tel.: +420 266 052 177; fax: +420 286 890 527; e-mail address: tomas@fzu.cz

Table 1. Chemical composition of the 54SiCr6 steel

Element	C	Mn	Si	P	S	Cr	Ni	Cu	Al
%	0.540	0.680	1.470	0.017	0.009	0.610	0.050	0.070	0.032

of the micro-hardness profile at the material cross-section, (iii) direct carbon content measurement by chemical or spectrographic analyses.

Alternatively, several *non-destructive* ways of similar detection were also suggested and tested. They are (i) eddy currents, eventually followed by the signal Fourier analysis [1, 2], (ii) Barkhausen noise [3], (iii) magneto-impedance approach [4], and (iv) ultrasonic attenuation [2]. It is one of the goals of this paper to show that Magnetic Adaptive Testing (MAT) is another candidate for non-destructive detection of decarburized layers on steel surfaces, a candidate that especially at some configurations shows an extremely high sensitivity.

In fact, characterization of the decarburization effect requires not only to measure its thickness but also to reflect any possible surface strengthening and/or degradation due to the usual later applied oxides-removing (Fe_2O_3, Fe_3O_4, FeO) processes like sand-blasting, pickling, and/or surface machining. These technologies bring surface residual stress and surface defects into the soft decarburized layer, which – in contrast to some other non-destructive methods – can be well reflected by a magnetic technique.

2. Experimental

2.1. Samples

The detrimental influence of decarburization is mainly felt in high strength steels with high content of carbon. We tested several types of commercial steel and eventually spring steel 54SiCr6 (CSN 14260) was chosen for the decarburization experiments discussed below. A detailed study of decarburization behaviour of the same steel 54SiCr6 during its reheating and cooling in ambient atmosphere was lately published in [5].

Thickness of the decarburized layer depends on time of the material exposure to air and on temperature of annealing. The decarburization behaviour of steel 54SiCr6 is shown in Fig. 1. Annealing and hardening of thin-cross-section steel 54SiCr6 are recommended to be carried out at temperatures between 710 and 850 °C.

According to written standards the condition +A (spheroidizing) of the steel 54SiCr6 corresponds to maximum Brinell hardness 253 HB, the condition +QT (heat treatment = quenching and tempering) enables $R_m = \langle 1470; 1770 \rangle$ MPa, and Vickers hardness HV = ⟨437; 507⟩.

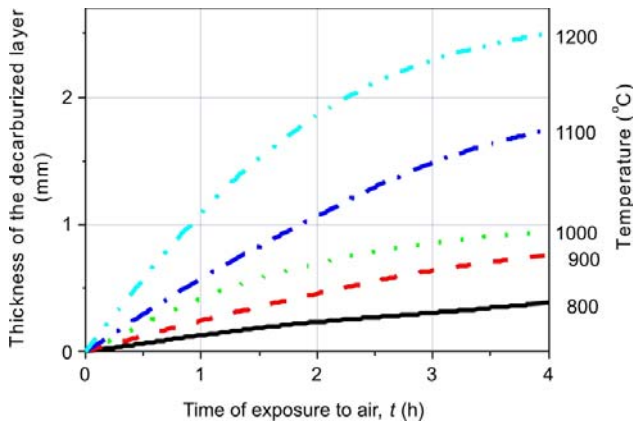

Fig. 1. Standard dependence of the thickness of the surface decarburized layer of steel 54SiCr6 on time of the material exposure to air at various temperatures (according to CSN 14260 standard specification).

Chemical composition of the 54SiCr6 steel used for our samples was measured by the Spectrumat GDS750, and it is shown in Table 1.

As the surface decarburization layers are generally more markedly detected in thin specimens, all samples used in the following experiments were produced from a 3 mm thick steel sheet. The shapes of the samples were rings (60/54/3 mm), annuli (60/24/3 mm), plates (110 × 30 × 3 mm^3) and rods (110 × 3 × 3 mm^3). As explained below, altogether more than 160 samples were used and tested in the following experiments.

2.2. Heat treatment

Majority of samples were *annealed in air* at temperature 800 °C. Always 36 samples (nine samples of each four sample shapes) were annealed for different time periods, namely for 1, 4, 8, and 20 h. The temperature was increased from room temperature to the final one during 1 h. Then the final temperature was kept constant for 1, 4, 8, and 20 h, respectively. The samples were then cooled in the furnace by 200 °C h^{-1} down to 600 °C, then cooling in the furnace continued with 100 °C h^{-1} down to 500 °C, and then the samples were removed from the furnace and cooled down to room temperature in stationary air.

In order to get reference samples *without* the decarburized layer but with a similar heat treatment of the

bulk material, other 36 samples (again nine samples of each shape) were annealed for 2 h in a *vacuum* furnace, using an equivalent heating and cooling regime.

2.3. Surface treatment

From each set of nine samples of each shape always three samples were left as grown, three were acid-pickled and three were sand-blasted, after the annealing. The surface treatment simulated the usual industrial processing of products, which substantially influence both their appearance and their fatigue properties. Figure 2 shows microphotographs of the three differently treated surfaces.

The *as-grown surfaces* were covered with oxides, which after 8 and 20 h of annealing had tendency to peel in scales.

The *pickling* removed the oxides chemically, and left the surface with enlarged crystallites of ferrite. Pickling was carried out by perpendicular suspension of specimens for 3 to 4 h into beakers with hydrochloric acid diluted 1 : 1 with water and inhibited with 3.5 g urotropine/litre.

The *sand-blasting* was performed manually with a nozzle by compressed air of 5 atm with SiO_2 sand grains sized 0.5–1 mm. Each sample area was treated from a distance of about 150–200 mm for maximum 5 s.

2.4. Magnetic Adaptive Testing (MAT)

MAT was applied to the samples in order to indicate presence and quantitative/qualitative properties of the decarburized surface layers. MAT belongs to the family of magnetic hysteresis testing methods. The *traditional* hysteresis magnetic test originates from measurement of *major* hysteresis loops of a series of samples, in which the investigated property – here the thickness of the decarburized layer – is varied and then one or more traditional magnetic variables (e.g. coercive force, H_C, remanent magnetic induction, B_R, maximum permeability, μ_{MAX}, and/or a few others), are monitored as they are modified by the magnitude of the investigated property – see e.g. [6, 7].

In contrast to this, MAT starts with measurement of *complex families of minor hysteresis loops* for each sample and picks up from a large pool of experimental data those data, which change with respect to the investigated property with the top sensitivity and reliability. Such an *adaptation* of the tests with respect to the actual experimental task makes the MAT substantially *more sensitive* than any type of the traditional hysteresis testing based on the single major loop only. Details of application of the MAT method can be found e.g. in [8].

The complex sets of data, which were collected for each sample in this paper, were actually families of differential permeability minor loops. Differential permeability, μ, is directly proportional to the signal induced in a pick-up coil when the sample is magnetized by a linearly sweeping magnetic field, F (see [8] for a detailed discussion). The amplitude, A_j, of minor loops in each family was step by step increased from

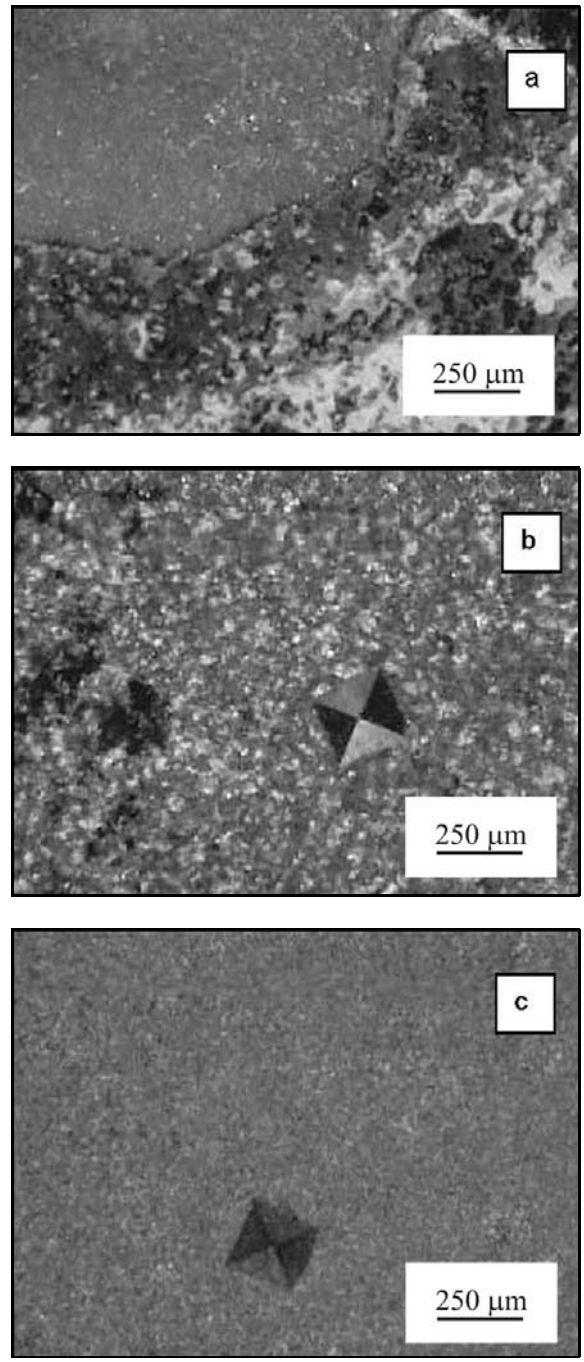

Fig. 2. Sample surfaces after different surface treatments. From up to down: (a) *as grown* (oxides forming scales), (b) *pickled* leaving the enlarged crystallites of ferrite, (c) *sand-blasted* forming the smoothest surface. The diagonal of the visible Vickers indents is approximately 250 μm.

Table 2. Vickers hardness and thickness of the surface layers after annealing at 800 °C

Annealed in		vacuum	air	air	air	air
Annealing time, t (h)		2	1	4	8	20
HV0.1	Surface	250	171	145	160	131
	Core	260	268	288	305	270
Thickness of the layers (μm)	Oxides	0	30	140	165	260
	Ferrite 100%	0	110	170	200	350
	Total L_{OC}: Ferrite 100 % + mixed ferrite/pearlite	**0**	**175**	**360**	**510**	**650**

a minimum up to the maximum, i.e. up to the major loop amplitude. The sweeping field, F, along each loop was then discretized with the same step, so that the whole data-pool measured for each sample, characterized by the known independent variable, ε_k, consisted of discrete values of differential permeability, $\mu(F_i, A_j, \varepsilon_k)$. The parameter ε_k means thickness of the decarburized layer L_{OC}, and/or time of exposition of the k-sample to the air during the annealing. A large set of general *μ-degradation functions*, $\mu(F_i, A_j, \varepsilon_k)$ – each specified by its field-coordinates-pair (F_i, A_j) – were defined for the pertinent series of samples, i.e. for all series of samples with the *same shape*, with the *same surface treatment* and with *different time of annealing*. Sensitivity and reliability of all degradation functions in each set was evaluated. The optimum degradation function was picked up as the calibration function for later magnetic non-destructive measurement of thickness of the decarburized layers in unknown samples of the proper type (the same material, the same shape, the same surface treatment, the same way of measurement). The calibration functions are plotted in the Section 3.5, and they demonstrate ability and sensitivity of the MAT method to indicate presence and properties of the decarburized layers in each case.

3. Results

3.1. Metallography of the annealed samples

After the annealing, the samples were investigated by metallography. Thickness of the surface layers was measured on the cross-sections as shown in Fig. 3 and also Vickers hardness HV0.1 was determined on the cross-sections. The measured thickness values and the limiting values of HV0.1 at the core and at the surface of the samples are summarized in Table 2.

Surface layers of oxides, of pure ferrite, and of mixture of ferrite with pearlite are clearly recognizable on the samples cross-section. This is shown in Fig. 3. The total thickness of the decarburization, L_{OC}, is defined as the distance from the metallic surface down to where the mixture of ferrite and pearlite comes visibly to the end.

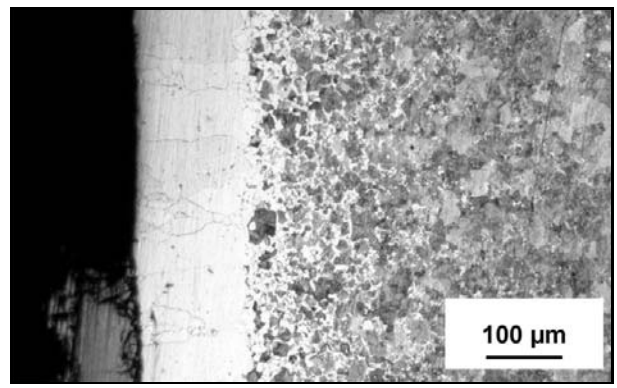

Fig. 3. Surface decarburization: metallography of cross-section of steel 54SiCr6 (CSN 14260) after 4 h exposition to air at 800 °C. The elemental division of the scale is 10 μm.

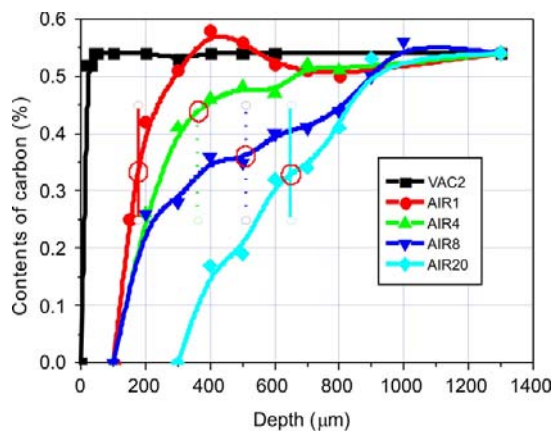

Fig. 4. Concentration of carbon measured by a microprobe in dependence on the depth from the metallic sample surface for samples annealed for 2 h in vacuum, and for 1, 4, 8, and 20 h in air atmosphere. Positions of L_{OC} as defined from the metallographic microphotographs are shown by the cross-points (red circles) of the curves with the vertical lines.

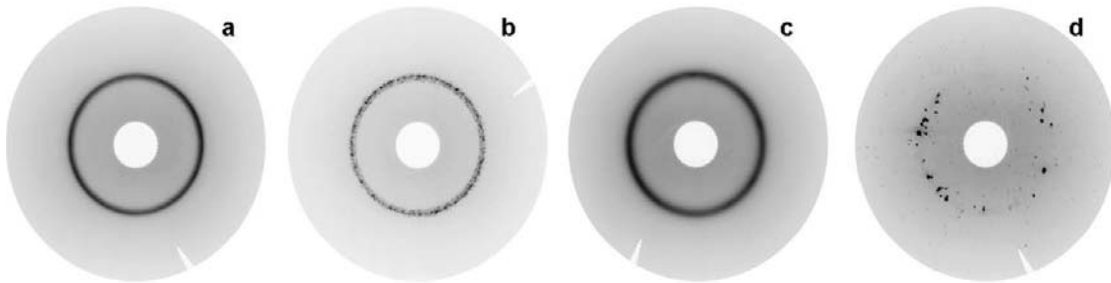

Fig. 5. The back-reflection XRD patterns of the 54SiCr6 steel samples. From left to right: (a) as-delivered sample, (b) sample annealed in vacuum for 2 h, (c) sample annealed in air for 8 h and then sand-blasted, (d) sample annealed in air for 8 h and then pickled in acid.

Table 3. Results of surface measurement of the residual stress

Sample and surface treatment	σ_{0° (MPa)	$\Delta\sigma_{0^\circ}$ (MPa)	σ_{90° (MPa)	$\Delta\sigma_{90^\circ}$ (MPa)
As-delivered sample with no treatment	38	5	−57	4
Vacuum annealed sample with no treatment	22	6	28	3
Air-annealed (8 h) sample after sand blasting	−282	11	−275	9

3.2. Carbon concentration

It is interesting to compare the metallographic definition, L_{OC}, of the decarburized layer with the measurement of the carbon content by an electron microprobe. Figure 4 presents results of such a measurement (the carbon content in the core material is 0.54 %, see Table 1) for the samples annealed in vacuum for 2 h, and in air for 1, 4, 8 and 20 h, respectively. As it shows, the L_{OC} thickness corresponds approximately to 2/3 of the full carbon concentration in the material core.

3.3. Surface X-ray diffraction analysis

Surface X-rays analysis was performed on disk-shaped samples processed in the same way as those prepared for the magnetic tests. The back-reflection XRD patterns [9] correspond to diffraction of the spectral doublet Cr Kα1, α2 on crystallographic planes {211} α-Fe, and they are presented in Fig. 5 for an as-delivered commercial material sheet of the steel 54SiCr6, for a sample annealed in vacuum for 2 h, and for samples annealed in air for 8 h and then sand-blasted or pickled, respectively. While the first three surfaces show isotropic fine-grained polycrystalline structure (the diffraction circle is continuous and has homogeneous intensity around its perimeter), in the case of the fourth specimen, where the surface oxides were removed by acid pickling, the discrete character of pattern, where diffraction spots are not located uniformly around perimeter, testifies about a coarse-grained material with suspicion of texture. The diffraction image of the samples after the annealing (but *before* the surface oxides were removed) does not contain the α-Fe diffraction at all and it is formed by superposition of diffraction lines of oxides Fe_2O_3 and Fe_3O_4 (not presented in Fig. 5). The ferrite crystals coarsen considerably after the acid pickling. This is the reason why the surface of the pickled samples cannot be used for determination of the surface residual stress by X-ray tensometry.

Results of the X-ray tensometry are presented in Table 3. The residual macroscopic stress was measured in two mutually perpendicular directions (σ_{0°, σ_{90°) selected randomly on the surfaces of the samples. The values $\Delta\sigma_{0^\circ}$ and $\Delta\sigma_{90^\circ}$ show the uncertainty of the measurements. The state of residual stresses in the surface layer of the as-delivered material showed slight anisotropy (Table 3), which was probably due to the sheet rolling during its production. This anisotropy was practically removed by annealing and the surface residual stress became uniform, very small and positive (tensile) – see the vacuum-annealed sample with no surface treatment in Table 3. High level of negative (compressive) isotropic residual stress in the sample surface layer was the result of the sand-blasting, as it is shown in the bottom row of Table 3. This effect is equivalent to mechanical toughening of the sample surface, which is clearly demonstrated at comparison of Vickers hardness HV10 determined on surfaces of the sand-blasted and acid-pickled samples (no mechanical toughening took place at the pickled samples) – see Fig. 6.

3.4. Variation in samples mass

Mass, G, of the samples was measured carefully

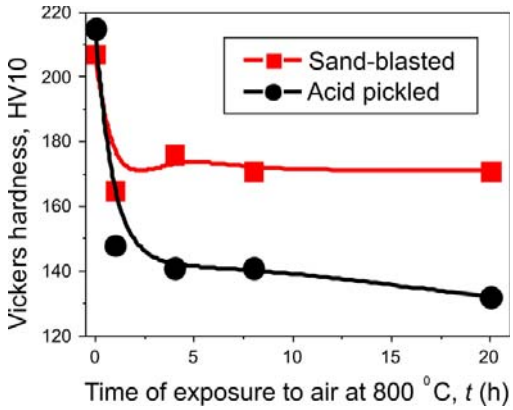

Fig. 6. Effect of mechanical toughening of the sand-blasted (■) samples surface as compared to the not-toughened acid pickled (●) samples.

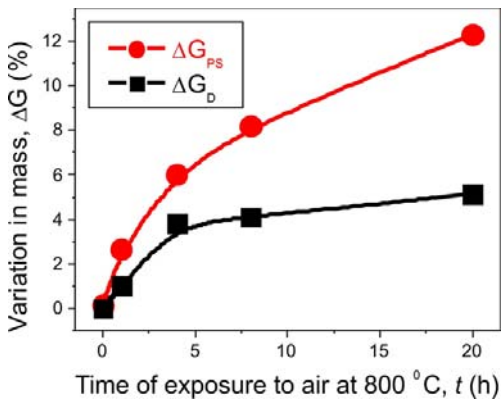

Fig. 7. Mass difference, ΔG_{PS} (●) between the as-grown samples and the acid pickled and/or sand-blasted samples, and mass difference, ΔG_{D} (■) between the as-grown samples and the samples as-delivered.

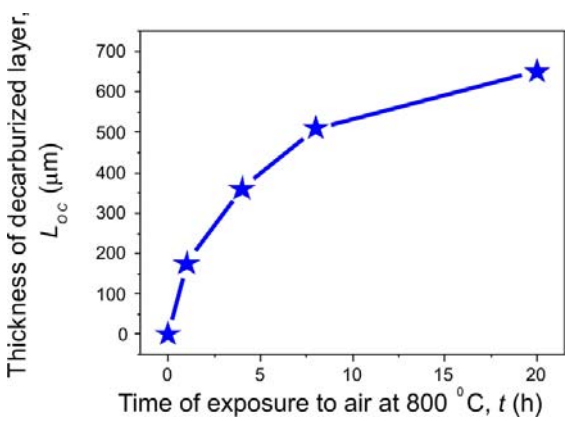

Fig. 8. Relation between time of the samples exposure to air at 800 °C and thickness of the total decarburized layer, L_{OC}, as it is given in Table 2.

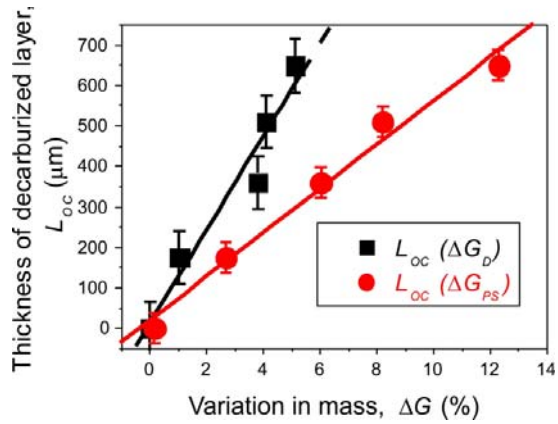

Fig. 9. Relation between variation of the mass differences ΔG_{D} (■) and ΔG_{PS} (●) and thickness of the decarburized layer, L_{OC}. The error bars show standard deviations of the linear fit of Eqs. (1) and (2).

with accuracy ± 0.05 g in all states and after all treatments. During the annealing in the air atmosphere, the air oxygen is captured by the iron at the surface, creating the mixed oxide layers of Fe_2O_3 and Fe_3O_4. The mass of each sample increases by this process, and the percentage of the mass increase can be seen in Fig. 7. The increase of the mass via the created oxides is characterized by the mass difference, ΔG_{D}, between the as-grown sample (i.e. with the oxides at the surface) and the sample as-delivered (i.e. without the oxides, before the annealing). The bottom curve, ΔG_{D}, in Fig. 7 represents thus the total mass of the captured oxygen. Another characterization is given by the mass difference, ΔG_{PS}, between the as-grown sample and the acid pickled and/or sand-blasted sample, which is presented by the top curve, ΔG_{PS}, in Fig. 7, and which thus represents the total mass of the oxides (as they were removed by pickling or by sand-blasting). Removal of the oxide layers both by pickling and by sand-blasting comes to the same result.

Evidently, increase of the samples mass is a unique, monotonous function of the time of annealing in air, similarly as is the increase in the thickness of the decarburized layer, L_{OC}. Total thickness of the decarburized layer, L_{OC}, can be thus determined from the variation of mass of the samples. Using the relation between the time of the samples exposure to air at 800 °C and the thickness of the decarburized layer, L_{OC}, (Table 2 and Fig. 8), and the dependence of Fig. 7, L_{OC} can be determined from the mass differences. For the applied steel sheet material 54SiCr6, 3 mm thick, annealed in air at 800 °C, empirical regression equations (1) and (2) are valid (Fig. 9), with the regression coefficients equal to 0.98 and 0.99, respectively:

$$L_{\mathrm{OC}}\ (\mu\mathrm{m}) = 116\Delta G_{\mathrm{D}}(\%) + 14, \quad k = 0.98, \qquad (1)$$

$$L_{\mathrm{OC}}\ (\mu\mathrm{m}) = 54\Delta G_{\mathrm{PS}}(\%) + 21, \quad k = 0.99. \qquad (2)$$

3.5. Magnetic Adaptive Testing

The MAT measurements were carried out with the aid of magnetizing and pick-up coils. The magnetically closed rings and annuli had the coils wound directly on each of them. The magnetically open plates and rods were measured in a short magnetizing solenoid with the pick-up coil positioned in its middle. For an easier measurement of the plates and rods, their magnetic circuit was artificially closed by a couple of passive soft yokes attached at the two opposite plane surfaces of the samples. In the case of rods, one more measurement was done, this time in a solenoid without any artificial closing of the magnetic circuit.

3.5.1. Variation of sensitivity due to samples shapes and to ways of measurement

The different experimental conditions affected substantially results of the measurements, which were mainly demonstrated by different sensitivity of the top-sensitive μ-degradation functions in each case. The most sensitive measurements were performed on the magnetically closed shapes of the samples (rings and annuli), and the thin rings were better than the flat annuli. Sensitivities of the μ-degradation functions measured on the open sample shapes of the plates and rods, with the passive yokes closing their magnetic circuits, were lower than those of the rings and annuli, and they were comparable with each other. Sensitivity of the μ-degradation functions of the rods, measured without any artificial closing of the magnetic circuit in the solenoid, was the lowest. However, even in the lowest sensitive case of the rod samples measured in the solenoid without the yokes, the curves were very well measurable. The top sensitive μ-degradation functions of the employed samples are plotted in Fig. 10 for the series of acid-pickled samples. A detail of Fig. 10, encompassing just the starting part of the curves up to the annealing time of 1 h (and/or the decarburized layer, $L_{\mathrm{OC}} \leq 200\,\mu$), demonstrates that even the lowest sensitive curve exceeds the signal change of more than 50 % between the rod sample before decarburization and after the one hour annealing – see Fig. 11.

3.5.2. Variation of sensitivity due to samples surface treatment

Different surface treatments of the samples after annealing in the air also affected results of their measurements. This fact is again best demonstrated by different sensitivity of the top-sensitive μ-degradation functions in each case. The ring samples were used

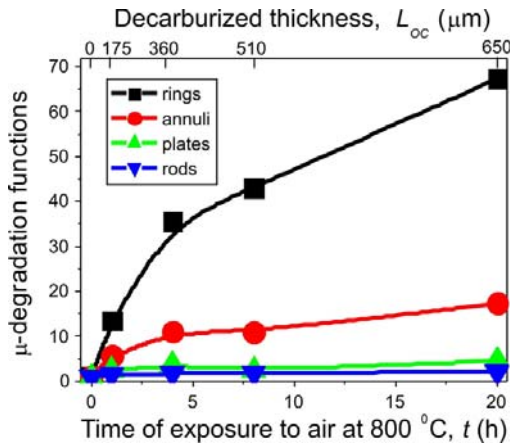

Fig. 10. Sensitivity of the best μ-degradation functions as it decreases with shape of the samples and with different ways of their magnetization. Oxide layers were removed by acid-pickling from the sample surfaces. The degradation function $\mu(F = 100\ \mathrm{A\,m^{-1}},\ A = 300\ \mathrm{A\,m^{-1}},\ t)$ (■) of the rings is more sensitive than that $\mu(F = 100\ \mathrm{A\,m^{-1}},\ A = 300\ \mathrm{A\,m^{-1}},\ t)$ (●) of the annuli. Plate samples measured with aid of the yokes give almost the same sensitivity of the optimum μ-degradation function $\mu(F = 467\ \mathrm{A\,m^{-1}},\ A = 1867\ \mathrm{A\,m^{-1}},\ t)$ (▲) as the rods $\mu(F = 1000\ \mathrm{A\,m^{-1}},\ A = 2500\ \mathrm{A\,m^{-1}},\ t)$ (▼) measured without the yokes.

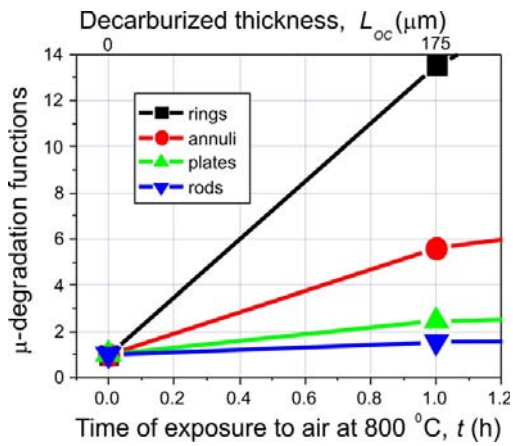

Fig. 11. Detail of the starting part of the curves of Fig. 10 shows that even the lowest sensitive curve (the magnetically open rod measured in the solenoid) exceeds the signal change of more than 50 % between the rod sample before decarburization and after the one hour annealing.

for this demonstration. Firstly, for the fact that measurement of ring samples does not need any aiding attached yokes and therefore it is not influenced by different magnetic contacts on differently treated sample surfaces. And secondly, for the best sensitivity of the MAT measurements on rings. Figure 12 shows comparison of the top sensitive μ-degradation functions measured on thin rings *with* the oxides on the surfaces (as grown), on rings *without* the oxide layers (removed

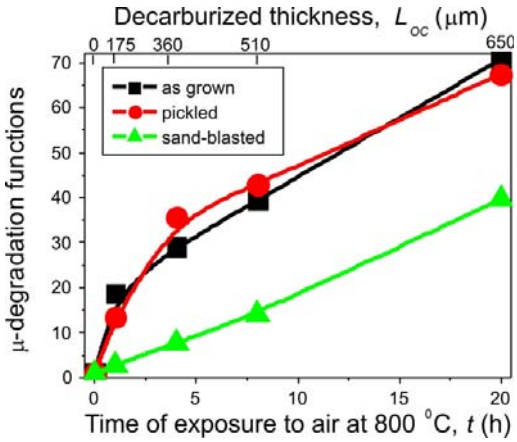

Fig. 12. Degradation functions $\mu(F = 100\,\mathrm{A\,m^{-1}},\ A = 300\,\mathrm{A\,m^{-1}},\ t)$ plotted here for the *ring* samples offer the top sensitivity of all the sample shapes. Surface treatment can change the sensitivity: (■) as-grown samples, (●) acid pickled samples, (▲) sand-blasted samples.

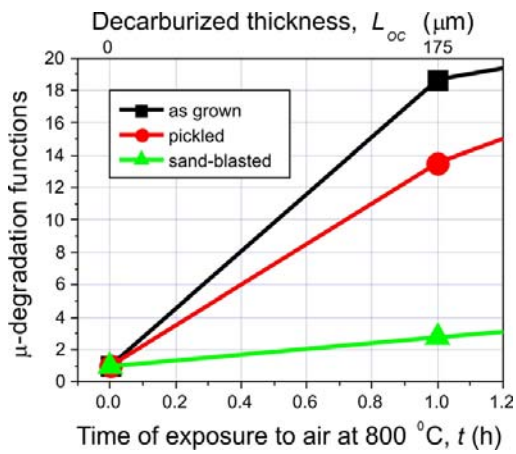

Fig. 13. Detail of the starting part of the curves of Fig. 12 shows that even after the surface treatment of the ring samples by sand blasting, the change of the signal exceeds 200 % between the ring sample before decarburization and after the one hour annealing.

by pickling the rings in the acid), and on rings *without* the oxide layers (removed by sand-blasting). Whereas the best μ-degradation functions of the ring samples *before and after the pickling* are practically the same, sand-blasting of the ring sample surfaces decreases the sensitivity by more than one half. A detail of Fig. 12, encompassing just the starting part of the curves up to the annealing time of 1 h (and/or the decarburized layer, $L_{OC} \leq 200\,\mu$), demonstrates, however, that even in the sand-blasted case the signal-change between the ring sample before decarburization and after the one hour annealing exceeds 200 % – see Fig. 13.

4. Discussion

The field coordinates of the μ-degradation functions are expressed in $\mathrm{A\,m^{-1}}$. This field value means the external magnetic field, F, applied on each sample by its magnetizing coil. The external field is varied linearly with time, but it is not identical with the internal magnetic field in the samples. The internal field in the samples is the external one decreased by the sample demagnetization field. The demagnetization is minimal at the rings and annuli, it can be artificially minimized during measurements of the plates and rods by the attached passive magnetic yokes, or it can be left as it is at measurements of the rods without application of the yokes. If the yokes are used for minimization of the demagnetization, they are attached to the sample surfaces as closely as possible. Quality of the magnetic contact between the sample and the yoke is very important, as any degradation of the magnetic contact influences the induced signal in exactly the same way as does the degradation of the sample material. In the discussed investigation of the decarburization, i.e. of the degradation of the samples due to changes at their surfaces, this can be a serious problem.

Rough, non-magnetic oxide layers develop on surfaces of the *as-grown* samples, which makes the use of yokes practically impossible. Removal of the oxides by *acid-pickling* helps. However, longer pickling for removal of thicker oxide layers makes the surfaces irregular and the surface ferrite crystallites get coarse. Quality of the magnetic contact with such surfaces often fluctuates, which makes the measured degradation functions scattered and the reading of degradation levels of unknown samples from the calibration curves is unreliable. Removal of the oxides by *sand-blasting* makes the surfaces optically smooth and the quality of the surface-to-surface *mechanical* contact between the yoke and the sand-blasted sample is constant. Unfortunately, however, this is not true for the quality of the *magnetic* contact. Surface of the sand-blasted samples is hardened by bombardment with the sand grains, and the hardening can differ according to variation in the applied sand-blasting processes. Besides, sand blasting modifies the surface toughness and decreases the sensitivity of the magnetic measurement – see Figs. 12 and 13.

Based on the above observations, best results can be expected from the measurements avoiding short-cutting of the magnetic flux by attached yokes, i.e. on samples with magnetically closed shape or on open samples magnetized in a solenoid without the yokes (the longer and thinner the sample, the better). Measurements employing attached yokes should be done very carefully and especially the calibration functions should be cautiously calculated by averaging from multiple measurements.

Starting point of all the μ-degradation functions in Figs. 10–13 is "1" at the zero level of the decarburized thickness. This results from normalization by values measured on the relevant samples (same shape, same treatment, same way of measurement) annealed for 2 h in vacuum. The vacuum-annealed samples were used for the normalization rather as the as-delivered material, because the core of the commercial material evidently did not go through the same unifying thermal process as our samples, which were all annealed for an appreciable time at 800 ℃. The as-delivered samples produced straight from the commercial material exhibited an unacceptable scatter of magnetic properties.

5. Conclusions

The inductive MAT measurement sensitively feels the surface decarburized layer, which is magnetically softer than the sample body. However, the sensitivity can be substantially choked down by surface stresses due to sand-blasting, and it strongly depends on the ways of magnetization of samples with different shape.

In spite of the relatively low sensitivity of flat, magnetically open samples magnetized with the yokes or without (as compared to the colossal sensitivity of the magnetically closed samples), their sensitivity reaches change of the signal by more than 100 % after 20 h of decarburization (and/or about 50 % after 1 h), which is more than enough for the indication of the surface decarburization layer.

It is also demonstrated, that it is possible to determine thickness of the decarburized layer, L_{OC}, by precise weighing of the samples before and after the annealing, and/or after the sand-blasting or pickling. Empirical equations – equivalent to our equations (1), (2) – obtained from such experiments on a reference series of samples can be applied only to the samples of the same kind as the reference ones, but the regression curves seem to be very linear and reliable. Thus precise weighing of the samples can be regularly recognized as an optional non-destructive way of measurement of the level of decarburization.

Acknowledgements

Laboratory of J. Švejcar at FMI VUT Brno performed chemical analysis of the used steel material and the measurement of the carbon concentration.

Financial support of the Czech Science Foundation (project No. 101/09/1323) is appreciated.

References

[1] MERCIER, D.—LESAGE, J.—DECOOPMAN, X.—CHICOT, D.: NDT&E International, *39*, 2006, p. 652. doi:10.1016/j.ndteint.2006.04.005

[2] HAK-JOON KIM—HO-SANG SHIN—DONG-YEOL KIM—SUNG-JIN SONG—SUNG-DUK KWON—TAKAGI, T.—UCHIMOTO, T.: In: Proceedings of the Sixth International Conference on Flow Dynamics, 2009. Sendai, Japan, Tohoku University (AFI/TFI-2009, CRF-16), p. 58.

[3] BLAOW, M.—EVANS, J. T.—SHAW, B. A.: Journal of Materials Science, *40*, 2005, p. 5517. doi:10.1007/s10853-005-4240-5

[4] HAO, X. J.—YIN, W.—STRANGWOOD, M.—PEYTON, A. J.—MORRIS, P. F.—DAVIS, C. L.: Scripta Materialia, *58*, 2008, p. 1033. doi:10.1016/j.scriptamat.2008.01.042

[5] DEJUN LI—ANGHELINA, D.—BURZIC, D.—ZAMBERGER, J.—KIENREICH, R.—SCHIFFERL, H.—KRIEGER, W.—KOZESCHNIK, E.: Steel Research International, *80*, 2009, p. 298.

[6] PARAKKA, A.—JILES, D. C.: NDT International, *21*, 1988, p. 311.

[7] BLITZ, J.: Electrical and magnetic methods of nondestructive testing. Bristol, Adam Hilger IOP Publishing, Ltd. 1991.

[8] TOMÁŠ, I.: Journal of Magnetism and Magnetic Materials, *268*, 2004, p. 178.

[9] GANEV, N.: X-ray diffraction analysis of decarburized surfaces. Research report 12 – 2009. Prague, Czech Technical University, Faculty of Nuclear Sciences and Physical Engineering (in Czech).